ACS SENSORS

pubs.acs.org/acssensors

Article

# Microfluidic Magneto Immunosensor for Rapid, High Sensitivity Measurements of SARS-CoV-2 Nucleocapsid Protein in Serum

Jiran Li and Peter B. Lillehoj*

Cite This: https://dx.doi.org/10.1021/acssensors.0c02561

Read Online

ACCESS | Metrics & More | Article Recommendations | Supporting Information

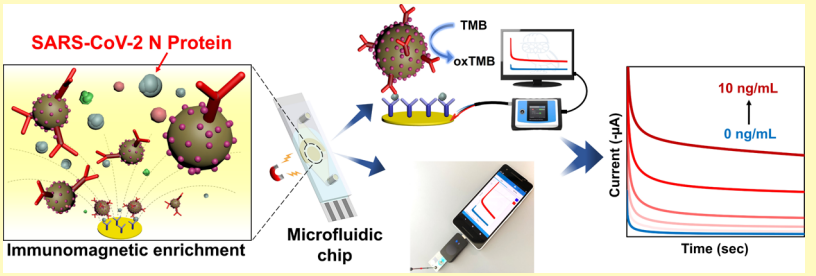


**ABSTRACT:** The COVID-19 pandemic has highlighted the importance and urgent need for rapid and accurate diagnostic tests for COVID-19 detection and screening. The objective of this work was to develop a simple immunosensor for rapid and high sensitivity measurements of SARS-CoV-2 nucleocapsid protein in serum. This assay is based on a unique sensing scheme utilizing dually-labeled magnetic nanobeads for immunomagnetic enrichment and signal amplification. This immunosensor is integrated onto a microfluidic chip, which offers the advantages of minimal sample and reagent consumption, simplified sample handling, and enhanced detection sensitivity. The functionality of this immunosensor was validated by using it to detect SARS-CoV-2 nucleocapsid protein, which could be detected at concentrations as low as 50 pg/mL in whole serum and 10 pg/mL in 5× diluted serum. We also adapted this assay onto a handheld smartphone-based diagnostic device that could detect SARS-CoV-2 nucleocapsid protein at concentrations as low as 230 pg/mL in whole serum and 100 pg/mL in 5× diluted serum. Lastly, we assessed the capability of this immunosensor to diagnose COVID-19 infection by testing clinical serum specimens, which revealed its ability to accurately distinguish PCR-positive COVID-19 patients from healthy, uninfected individuals based on SARS-CoV-2 nucleocapsid protein serum levels. To the best of our knowledge, this work is the first demonstration of rapid (<1 h) SARS-CoV-2 antigen quantification in whole serum samples. The ability to rapidly detect SARS-CoV-2 protein biomarkers with high sensitivity in very small (<50 $\mu$L) serum samples makes this platform a promising tool for point-of-care COVID-19 testing.

**KEYWORDS:** *microfluidic, immunosensor, electrochemical, SARS-CoV-2, nucleocapsid protein, COVID-19*

The current coronavirus disease (COVID-19) pandemic is widely considered one of the worst public health crises of the 21st century, with >50 million reported cases and >1 million fatalities worldwide occurring within 1 year after the virus was identified in Wuhan, China, in December 2019.[1] Nucleic acid testing based on reverse transcription-polymerase chain reaction (RT-PCR) has been the primary method of detecting severe acute respiratory syndrome coronavirus 2 (SARS-CoV-2), the virus that causes COVID-19. While PCR-based tests are highly specific for SARS-CoV-2, their accuracy is influenced by several factors, such as variations in the sample collection process and the persistence of viral RNA in the nasal cavity/throat weeks after infection and recovery, leading to false-negative/false-positive test results.[2−5] In addition, RT-PCR involves multiple sample processing steps (e.g., nucleic acid extraction, purification, and amplification), making it tedious and time-consuming (∼3−6 h), requires expensive (> $10,000) PCR instrumentation, and needs to be performed in a laboratory setting, making it poorly suited for large-scale testing. Recently, there has been a push to develop serological tests for COVID-19 that detect immune or viral proteins in the blood of infected individuals. Serological specimens are generally more stable than viral RNA and tend to have less variations than nasopharyngeal or oropharyngeal viral RNA specimens because proteins are uniformly distributed in the blood, minimizing the likelihood of false-negative test results.[6]

Current efforts to develop serological tests for COVID-19 are largely based on the detection of SARS-CoV-2 immunoglobulin G and M (IgG and IgM) antibodies using enzyme-linked immunosorbent assay (ELISA)[2,7−10] or lateral

Received: December 7, 2020
Accepted: February 17, 2021

flow immunoassays (LFAs).[10,11] While antibody tests have shown to be useful in identifying individuals with prior COVID-19 infections, it can take 2−3 weeks for viral-specific antibodies to be produced after infection,[12] limiting their utility for early-stage disease detection. In contrast, antigen tests enable the detection of viral proteins that appear at the onset of symptoms. A clinical study showed that SARS-CoV-2 nucleocapsid (N) protein could be detected in the serum of COVID-19 patients (PCR-positive) with a sensitivity and specificity of 92 and 97%, respectively.[13] In another study, SARS-CoV-2 spike (S1) and N proteins were detected in the plasma of COVID-19 patients at concentrations ranging from ∼8 to 20,000 and ∼0.8 to 1700 pg/mL, respectively.[14] These clinical studies demonstrate that quantitative measurements of SARS-CoV-2 antigens, such as N and S1 proteins, in serum/plasma are useful for accurate and early detection of COVID-19. While immunoassays (ELISA, Simoa) for quantifying SARS-CoV-2 antigens are commercially available, they involve multiple liquid handling steps (e.g., sample dilution, plate washing, etc.) and lengthy incubation (∼3−4 h in total) and need to be performed in a laboratory setting, limiting their usefulness for large-scale testing. Currently, only two antigen tests (Sofia 2 SARS Antigen FIA and BD Veritor System) have been approved by the FDA for the detection of N protein in nasopharyngeal/nasal swab samples. However, these tests only provide qualitative results and lack the sensitivity needed to detect low levels of SARS-CoV-2 antigens in the plasma/sera of COVID-19 patients.

Several groups have recently developed immunosensors for rapid quantification of SARS-CoV-2 antigens in biofluids. Fabiani et al. demonstrated the detection of SARS-CoV-2 S1 and N proteins at concentrations as low as 19 ng/mL and 8 ng/mL, respectively, in saliva using an electrochemical immunosensor.[15] Tan et al. developed a microfluidic chemiluminescent ELISA platform that could detect SARS-CoV-2 S1 and N proteins in 10× diluted serum in 40 min.[16] Torrente-Rodríguez et al. reported a multiplexed electrochemical immunoassay capable of detecting SARS-CoV-2 N protein and SARS-CoV-2 S1 IgG and IgM in 100× diluted serum samples.[17] While these immunosensors were successful in measuring SARS-CoV-2 antigens in biofluids samples, they could not achieve high sensitivity (pg/mL) or required high sample dilution.

In this work, we demonstrate for the first time rapid (<1 h), high sensitivity measurements of SARS-CoV-2 N protein in whole (undiluted) serum. This unique immunosensor utilizes dually-labeled magnetic nanobeads (DMBs) for on-chip immunomagnetic enrichment and signal amplification. Several assay parameters, including the antibody pair, the volume ratio of the sample to magnetic beads, the magnetic enrichment time, and the incubation time, were optimized to enhance the detection sensitivity. We show the capability of this immunoassay to detect SARS-CoV-2 N protein in undiluted human serum samples in <1 h with pg/mL sensitivity. We also demonstrate the detection of SARS-CoV-2 N protein in serum samples using a smartphone-based diagnostic device that can achieve high sensitivity and reproducibility. Lastly, we demonstrate the utility of this platform for accurately detecting COVID-19 infection by performing measurements of clinical serum specimens from COVID-19 patients and healthy, uninfected individuals.

## EXPERIMENTAL SECTION

**Biochemicals and Reagents.** Dimethyl sulfoxide (DMSO), phosphate-buffered saline (PBS, pH 7.4), (ethylenedinitrilo)-tetraacetic acid (EDTA), 2-Iminothiolane hydrochloride, human serum (from male AB-clotted whole blood), and 3,3′,5,5′-tetramethylbenzidine (TMB) substrate (supersensitive) were purchased from Sigma-Aldrich (St Louis, MO). *N*-(3-Dimethylaminopropyl)-*N*′-ethylcarbodiimide (EDC) and *N*-hydroxysuccinimide (NHS) were obtained from Thermo Fisher Scientific (Waltham, MA). StabilBlock immunoassay stabilizer, StabilCoat Plus immunoassay stabilizer, StabilZyme HRP stabilizer, and MatrixGuard assay diluent were purchased from SurModics, Inc. (Eden Prairie, MN). Carboxylated magnetic nanobeads (200 nm) were purchased from Ademtech (Pessac, France). SARS-CoV-2 nucleocapsid protein was obtained from Advaite, Inc. (Malvern, PA). Mouse monoclonal SARS-CoV/SARS-CoV-2 nucleocapsid antibody [6H3] (GTX632269), rabbit polyclonal SARS-CoV-2 nucleocapsid antibody (GTX135357), SARS-CoV-2 nucleocapsid antibody pair [HL5410/HL455-MS] (GTX500042), and horseradish peroxidase (HRP)-conjugated rabbit monoclonal SARS-CoV-2 nucleocapsid antibody [HL448] (GTX635686-01) were purchased from GeneTex (Irvine, CA). Human monoclonal anti-SARS-CoV-2 nucleocapsid antibody [SQab20177] (ARG66735), MERS-CoV nucleocapsid recombinant protein (His-SUMO tagged, *N*-ter), and SARS-CoV nucleocapsid recombinant protein (His-SUMO tagged, *N*-ter) were purchased from Arigo (Taiwan, ROC). Recombinant SARS-CoV-2 spike glycoprotein RBD (ab273065) was obtained from Abcam (Cambridge, MA). De-identified serum samples obtained from healthy volunteers and COVID-19 patients were purchased from BioIVT (NY, USA).

**Preparation of Dually-Labeled Magnetic Nanobeads.** DMBs were prepared by dispersing 1 mg of carboxylated magnetic nanobeads in 400 μL of MES buffer (pH 5.0, 25 mM) and washing thrice (gentle agitation for 5 min followed by magnetic separation for 5 min and subsequent removal of the supernatant). Next, 100 μL of MES buffer containing HRP and detection antibody (dAb) at a 400:1 molar ratio was mixed with the nanobeads preactivated with 10 mg/mL of EDC/NHS and incubated overnight at room temperature. After washing with PBS and blocking of nonspecific binding sites with a StabilCoat Plus stabilizer, the DMBs were dispersed in 400 μL of StabilZyme HRP stabilizer to a final concentration of 2.5 mg/mL and used immediately or stored at 4 °C for up to 2 weeks.

**Preparation of Immunosensors.** Screen-printed gold electrode (SPGE) sensors were obtained from Metrohm AG (Herisau, Switzerland). Capture antibodies (cAbs) were first thiolated by incubating 100 μL of cAb at 50 μg/mL with 100-fold molar excess of 2-iminothiolane in PBS containing 2 mM of EDTA for 1 h at room temperature, followed by centrifugation for 25 min at 13,800 g to remove excess reagents. Thiolated cAbs were immobilized on the SPGE sensor by incubating 6 μL of cAb solution at 50 μg/mL on the working electrode (WE) for 2 h at room temperature, followed by rinsing with PBS and gently drying with purified $N_2$. StabilBlock stabilizer solution was dispensed on the sensor and dried at room temperature to passivate the surface and enhance the stability of the immobilized cAb. Sensors were stored at room temperature in a desiccator (<15% RH) and used within 1 week.

**Fabrication of Microfluidic Chips.** The microfluidic chips consist of a 100 μm-thick polyethylene terephthalate (PET) film (McMaster-Carr) stacked with a 3 mm-thick poly(methyl methacrylate) (PMMA) cartridge on top of an immunosensor. Microchannels and microfluidic components were designed using AutoCAD software (Autodesk, Inc.). Microchannels, inlets, and outlets were generated in the PET and PMMA layers using a $CO_2$ laser cutter (Universal Laser Systems, Scottsdale, AZ). The PET film, PMMA cartridge, and SPGE sensor were bonded together using double-sided adhesive film (Adhesives Research, PA).

**Electrochemical Measurements.** Electrochemical measurements were performed at ambient conditions using either a PalmSens4 potentiostat connected to a desktop PC or a Sensit Smart potentiostat connected to a Google Pixel 2 smartphone. Prior


https://dx.doi.org/10.1021/acssensors.0c02561
ACS Sens. XXXX, XXX, XXX−XXX

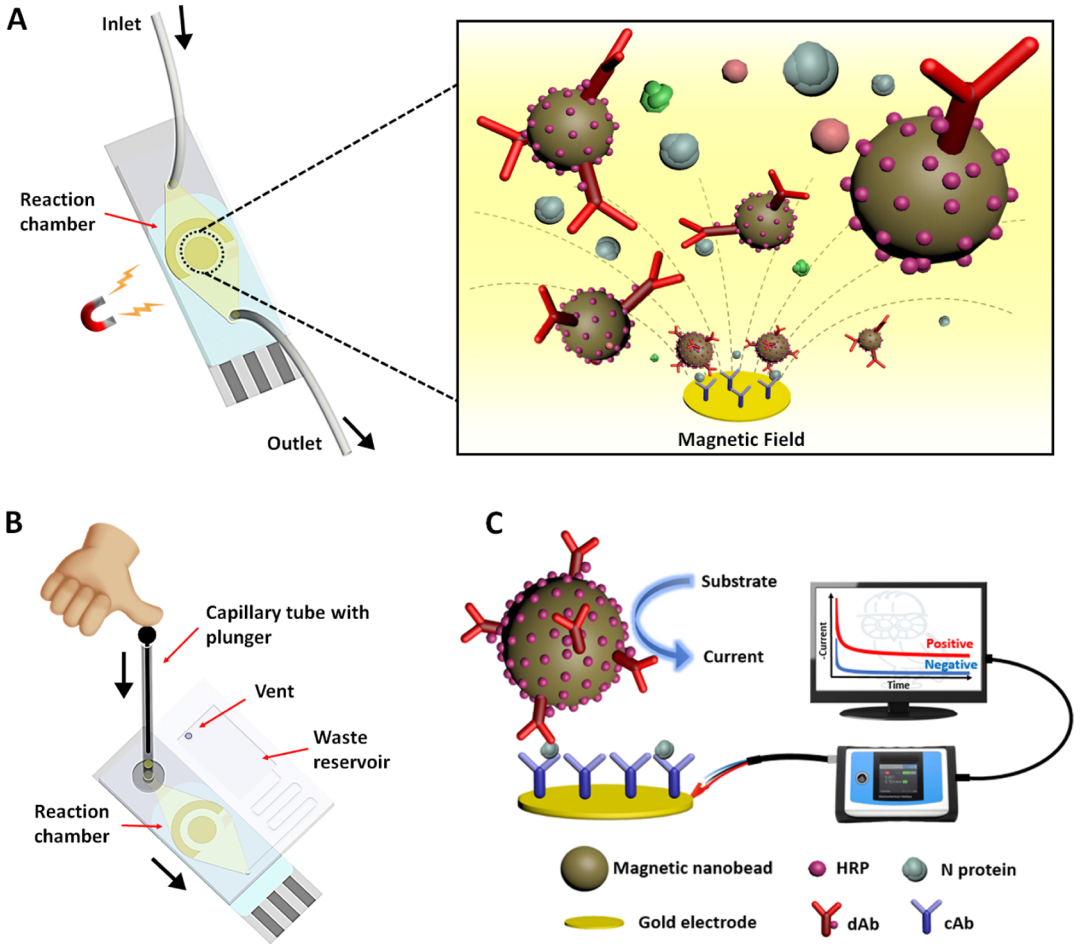


**Figure 1.** Schematic illustrations of (A) microfluidic immunosensor chip highlighting the magnetic concentration of DMBs to the sensor surface, (B) microfluidic immunosensor chip for the smartphone-based diagnostic device, and (C) experimental setup and electrochemical sensing scheme using the PalmSens4-based sensing platform.

to measurements, 2.5 $\mu$L of DMB solution was mixed with 50 $\mu$L of serum spiked with N protein or clinical serum specimens, vortexed for 5 s, and dispensed into the microfluidic chip. Spiked serum samples were either used as is or diluted 5× in MatrixGuard assay diluent. For measurements using the PalmSens4 and desktop PC, the sample was infused through the chip for 30 s at 100 $\mu$L/min using a syringe pump (KD Scientific, MA). For measurements using the smartphone-based sensing device, the sample was dispensed into the chip using a capillary tube and plunger (Abbott). The microfluidic chip was then placed on a 4 mm neodymium magnet (McMaster-Carr) for 1 min to concentrate the DMBs on the WE and incubated in the dark for either 50 min for whole serum samples or 25 min for diluted serum samples. Measurements of clinical serum specimens were performed by diluting samples 5× in an assay diluent (to conserve the sample for replicate measurements), followed by immunomagnetic enrichment and incubation for 25 min. A wash buffer (1× PBS containing 0.05% Tween-20) was flushed through the chip for 4 min at 100 $\mu$L/min, followed by a TMB substrate for 1 min at 100 $\mu$L/min for measurements using the PalmSens4 and desktop PC. For measurements using the smartphone-based sensing device, a 1 cc plastic syringe (Thermo Fisher Scientific) was inserted into the inlet of the microfluidic chip and used to purge the sample from the chip, followed by the sequential application of 80 $\mu$L of wash buffer and 80 $\mu$L of TMB substrate into the chip using fresh capillary tubes and plungers. After 2 min, chronoamperometric measurements were performed by applying a bias potential of −0.2 V (vs Ag/AgCl) for 100 s. Current values were averaged over the final 5 s of chronoamperograms.

## RESULTS AND DISCUSSION

**Design of the Microfluidic Chip.** The integration of this immunosensor on a microfluidic platform offers several advantages over open well format immunoassays. Specifically, the recommended working volume for a standard 96-well microtiter plate is 100−200 $\mu$L, whereas our microfluidic immunosensor requires only 25 $\mu$L of sample and 80 $\mu$L of reagent per measurement. In addition, sample processing and liquid handling for open well format assays involve multiple pipetting steps, which are tedious and time-consuming. In contrast, sample processing (immunomagnetic enrichment) and liquid handling (sensor washing) are performed directly on our microfluidic chip, which minimizes the labor and time required for each measurement, facilitating its use for point-of-care testing. Lastly, the integration of immunosensors with microfluidics has been shown to significantly reduce the time for antibody−antigen reactions and enhance the detection sensitivity compared with open well format immunoassays.[18,19] We briefly studied the analytical performance of our microfluidic immunosensor compared with an open-well immunosensor and observed that the amperometric currents and signal-to-background (S/B) ratios generated from the microfluidic immunosensor were 3−4× higher than those generated from the open-well immunosensor (Supporting Information Figure S1).


https://dx.doi.org/10.1021/acssensors.0c02561
ACS Sens. XXXX, XXX, XXX−XXX

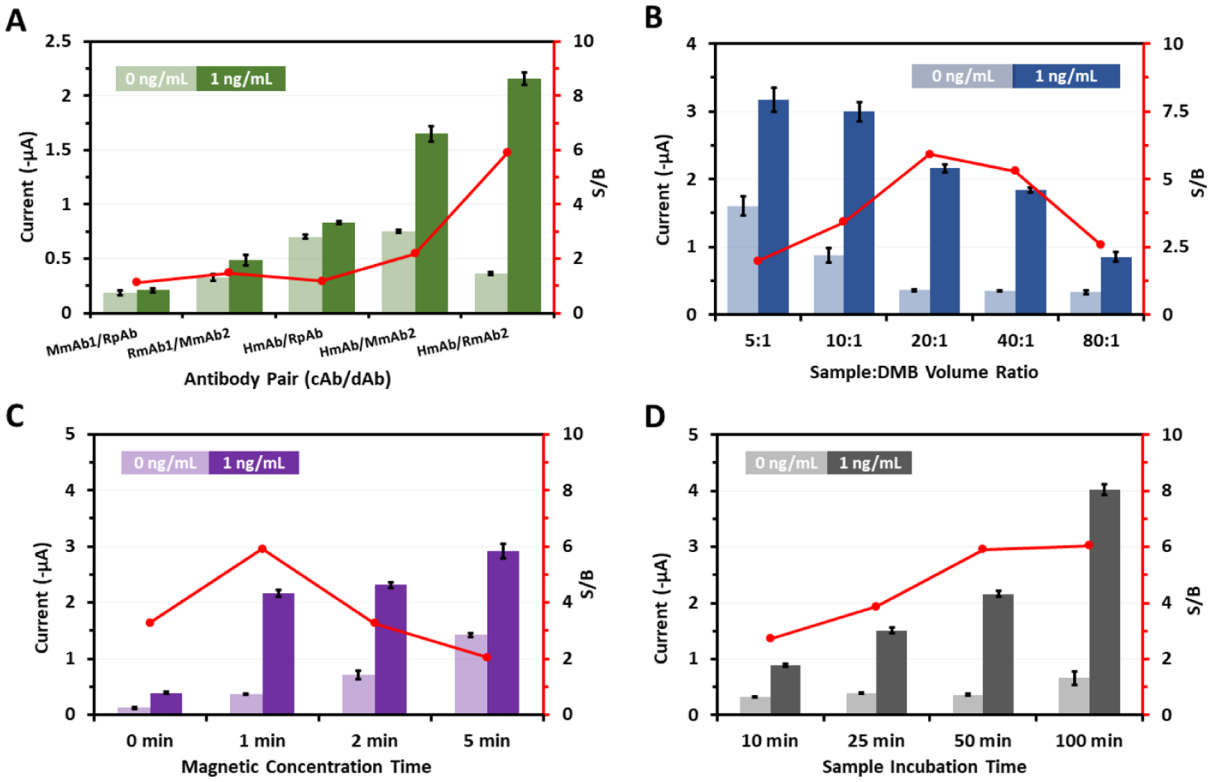


**Figure 2.** (A) Amperometric currents generated from undiluted serum samples spiked with SARS-CoV-2 N protein at 0 and 1 ng/mL and corresponding S/B ratios using immunosensors with five different SARS-CoV-2 N protein antibody pairs. Measurements were performed using magnetic enrichment and incubation times of 1 and 50 min, respectively. (B) Amperometric currents generated from undiluted serum samples spiked with SARS-CoV-2 N protein at 0 and 1 ng/mL and corresponding S/B ratios with varying sample/DMB volume ratios. Measurements were performed using magnetic enrichment and incubation times of 1 and 50 min, respectively (C) Amperometric currents generated from undiluted serum samples spiked with the SARS-CoV-2 N protein at 0 and 1 ng/mL and corresponding S/B ratios with varying magnetic enrichment times and a 50 min sample incubation duration. (D) Amperometric currents generated from undiluted serum samples spiked with SARS-CoV-2 N protein at 0 and 1 ng/mL and corresponding S/B ratios with varying incubation times and 1 min of magnetic enrichment. Each bar represents the mean ± standard deviation (SD) of three separate measurements obtained using new sensors.

Different microfluidic chips were designed for measurements using the PalmSens4-based sensing platform and the smartphone-based diagnostic device. For measurements using the PalmSens4, the chip consists of a 400 $\mu$m-high reaction chamber encompassing the immunosensor connected to the inlet and outlet (Figure 1A). The microfluidic chip for measurements using the Sensit Smart and smartphone consists of a 400 $\mu$m-high reaction chamber encompassing the immunosensor connected to a 9 × 12 mm waste reservoir via a 500 $\mu$m-wide serpentine channel (Figure 1B) and an air vent. A rubber gasket is installed at the inlet of the chip to facilitate the insertion of the capillary tube and prevent leaking.

**Design of the Electrochemical Magneto Immunoassay.** Prior works have demonstrated the use of antibody-labeled magnetic beads for immunomagnetic enrichment and signal amplification, enabling sensitive analyte detection in complex biofluids.[20,21] Otiena et al. reported a microfluidic magneto immunoassay for multiplexed detection of a parathyroid hormone-related peptide and peptide fragments in serum.[22] While this assay was capable of performing ultrasensitive protein measurements, the experimental setup involves multiple components (e.g., magnetic stirrer, sample injector, syringe pump, switching valve, etc.), hindering its use for point-of-care applications. In this work, we utilize a simple and rapid (1 min) method for immunomagnetic enrichment using a low-cost neodymium magnet. The serum sample is premixed with DMBs prior to loading into the microfluidic chip, which is carried out using either a syringe pump or capillary tubes and plungers (for the smartphone-based device). If the sample contains the target antigen, it binds to the DMB and forms a DMB−antigen immunocomplex. When the chip is placed on the magnet, a magnetic field is generated, causing the DMB−antigen immunocomplexes to rapidly migrate to the sensor surface where they subsequently bind to the cAb-immobilized WE (Figure 1A). In the presence of the TMB substrate, the HRP-coated DMBs catalyze the reduction of TMB upon application of a bias potential, which generates an amperometric current that is proportional to the concentration of target antigen attached to the sensor surface (Figure 1C). If the sample does not contain the target antigen, then the DMBs are washed away from the sensor surface and a negligible electrochemical signal is generated upon the application of a bias potential.

**Optimization of Assay Parameters.** Several assay parameters, including the antibody pair, sample to DMB solution volume ratio, magnetic enrichment time, and incubation time, were optimized to enhance the analytical performance of this immunosensor for SARS-CoV-2 N protein detection. One of the most important parameters that affects the performance of immunoassays is the antibody affinity toward the target antigen. There are numerous SARS-CoV-2 N protein antibodies that are commercially available, and each


https://dx.doi.org/10.1021/acssensors.0c02561
ACS Sens. XXXX, XXX, XXX−XXX

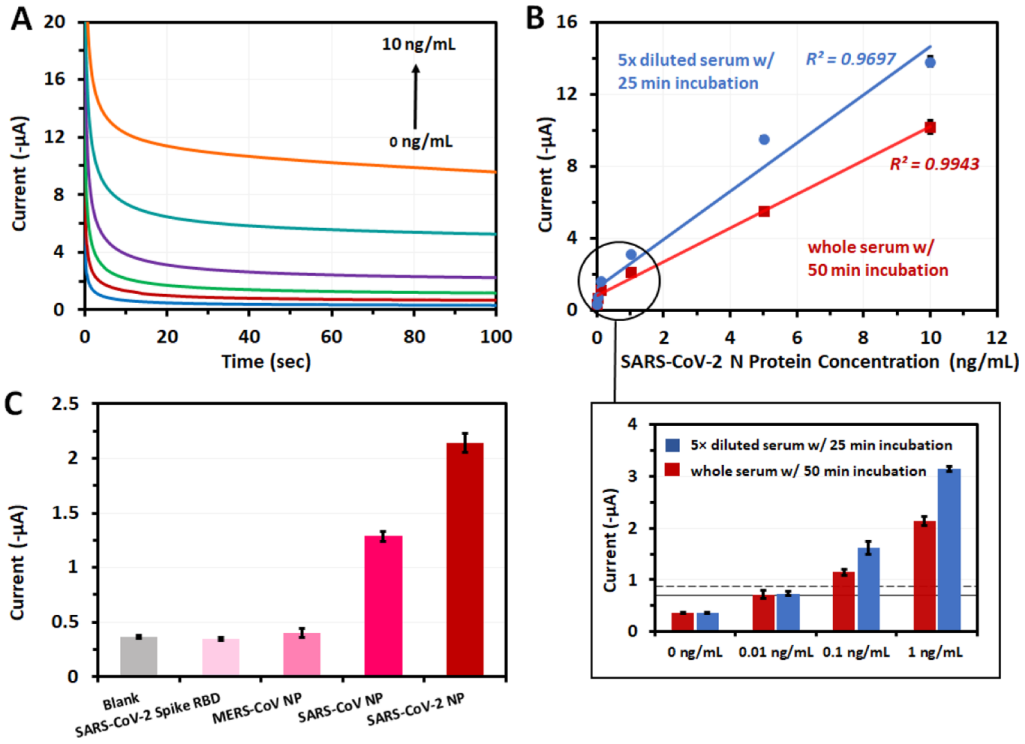


**Figure 3.** (A) Chronoamperograms generated from whole serum samples spiked with SARS-CoV-2 N protein at varying concentrations. (B) Calibration plots based on amperometric currents at 100 s for whole serum samples with 50 min incubation and 5× diluted serum samples with 25 min incubation. Each data point represents the mean ± SD of three separate measurements obtained using new sensors. The inset shows amperometric currents for samples containing SARS-CoV-2 N protein from 0 to 1 ng/mL. Each bar represents the mean ± SD of three separate measurements obtained using new sensors. The dashed and solid lines correspond to the lower LOD for measurements of whole serum and 5× diluted serum, respectively. (C) Amperometric currents generated from serum samples containing SARS-CoV-2 N protein, SARS-CoV N protein, MERS-CoV N protein, SARS-CoV-2 Spike RBD protein and nonspiked serum (blank control). Each bar represents the mean ± SD of three separate measurements obtained using new sensors.

one possesses a specific antigenicity to the SARS-CoV-2 N protein. Therefore, to determine the optimal antibody pair for our immunosensor, we performed measurements of SARS-CoV-2 N protein spiked in whole serum at 0 and 1 ng/mL using SPGE sensors with five different antibody pairs. The cAbs were immobilized on the WE of the sensors as described in "Preparation of Immunosensors," and dAbs were conjugated with DMBs as described in "Preparation of Dually-Labeled Magnetic Nanobeads". The amperometric signals generated using the five antibody pairs are presented in Figure 2A. Antibody pairs consisting of a mouse or rabbit cAb generated very low amperometric signals (<0.5 $\mu$A) and low S/B ratios of <2, indicating poor antigenicity to SARS-CoV-2 N protein because they are raised against nonhuman species. Amperometric signals generated from immunosensors using a human monoclonal cAb were significantly larger than those generated from sensors using a nonhuman monoclonal cAb; however, when paired with a mouse monoclonal antibody or rabbit polyclonal antibody as the dAb, a very high background signal was observed, resulting in negligible improvement in the S/B ratio. Lastly, we evaluated the use of a rabbit monoclonal antibody conjugated with HRP as the dAb, which generated a large electrochemical current with a low background signal, resulting in a S/B ratio of ~6. Thus, a human monoclonal cAb and a HRP-conjugated rabbit monoclonal dAb were selected as the optimal antibody pair and used for subsequent assay optimization experiments.

The sample to DMB solution ratio was optimized by performing measurements of serum samples spiked with increasing concentrations of SARS-CoV-2 N protein using varying volumes of DMB solution. As shown in Figure 2B, the amperometric signal is correlated with the sample/DMB volume ratio where measurements using higher sample/DMB volume ratios resulted in lower electrochemical currents. However, measurements using low sample/DMB volume ratios (<10:1) resulted in high background signals and low S/B ratios (<3.5) due to an excessive amount of DMBs, which increases the likelihood of nonspecific binding of DMBs on the sensor. As the sample/DMB volume ratio increases, the background signal decreases until a sample/DMB volume ratio of 20:1, after which point, the background signal remains constant. The largest S/B ratio (~5.5) was obtained using a sample/DMB volume ratio of 20:1, which was selected as the optimal volume ratio.

Experiments were also performed to optimize the magnetic enrichment time by detecting SARS-CoV-2 N protein spiked in serum samples at 0 ng/mL and 1 ng/mL with varying durations of magnetic enrichment (Figure 2C). With no magnetic enrichment, a very low (<0.5 $\mu$A) amperometric signal is generated at 1 ng/mL, resulting in a S/B ratio of ~3. Applying magnetic concentration for 1 min resulted in a significant increase in the amperometric signal by 5×, compared with no magnetic enrichment, with a minimal rise in the background signal (S/B ratio of ~6). These results demonstrate that the migration of DMBs to the sensor surface is significantly enhanced in the presence of a magnetic field, which facilitates the attachment of antigen−DMB immunocomplexes on the cAb-coated immunosensor. Applying


https://dx.doi.org/10.1021/acssensors.0c02561
ACS Sens. XXXX, XXX, XXX−XXX

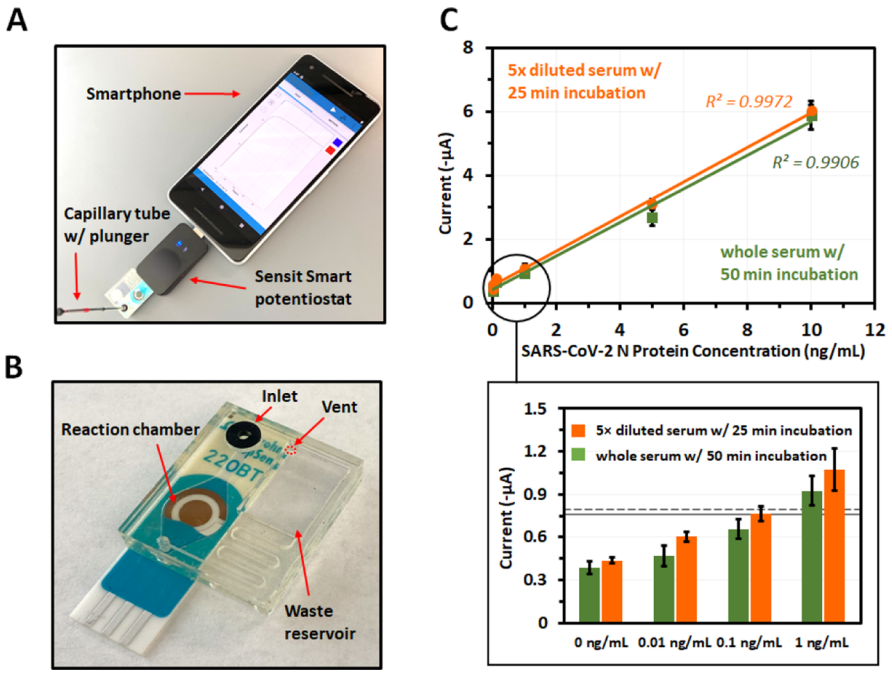


**Figure 4.** (A) Smartphone-based diagnostic device for electrochemical measurements of SARS-CoV-2 N protein. (B) Microfluidic immunosensor chip consisting of a cAb-coated SPGE sensor and PET−PMMA cartridge. (C) Calibration plots based on amperometric currents at 100 s for whole serum samples with 50 min incubation and 5× diluted serum samples with 25 min incubation. Each data point represents the mean ± SD of three separate measurements obtained using new sensors. The inset shows amperometric currents for samples containing SARS-CoV-2 N protein from 0 to 1 ng/mL. Each bar represents the mean ± SD of three separate measurements obtained using new sensors. The dashed and solid lines correspond to the lower LOD for measurements of whole serum and 5× diluted serum, respectively.

magnetic concentration for >1 min resulted in a minimal rise in the amperometric signal with a more pronounced increase in the background signal, causing the S/B ratio to decrease. We hypothesize that the increase in the background signal with longer magnetic enrichment durations (>1 min) is due to the accumulation and subsequent trapping of unbound DMBs on the coarse SPGE sensor surface, which cannot be completely removed with laminar flow rinsing.

The last parameter that was studied was the post-immunomagnetic enrichment incubation time. Measurements were performed using serum samples spiked with SARS-CoV-2 N protein at 0 and 1 ng/mL using a magnetic concentration duration of 1 min with varying incubation times. As shown in Figure 2D, longer incubation times resulted in higher S/B ratios until a steady state was reached at 50 min. While larger amperometric signals can be generated with incubation times longer than 50 min, the background signal also increases proportionally, leading to a negligible improvement in the S/B ratio. Therefore, 50 min was selected as the optimal incubation time.

**Detection of SARS-CoV-2 N Protein in Serum.** Measurements of whole serum and 5× diluted serum spiked with increasing concentrations of SARS-CoV-2 N protein were carried out to assess the analytical performance of this immunosensor. Chronoamperograms generated from whole serum samples containing SARS-CoV-2 N protein from 0 to 10 ng/mL are shown in Figure 3A, which show a positive correlation between the amperometric current and SARS-CoV-2 N protein concentration. Calibration plots based on amperometric currents at 100 s for whole serum and 5× diluted serum are presented in Figure 3B. The response of this sensor is highly linear for whole serum with a $R^2$ correlation coefficient of 0.9943. The linearity of the calibration curve for 5× diluted serum ($R^2$ = 0.9697) is lower than that for whole serum, which is likely due to the use of a supersensitive TMB substrate, resulting in limited reaction kinetics at higher (>1 ng/mL) analyte concentrations. While the use of an alternative TMB substrate could improve the linearity, this could lead to a less desirable analytical performance with a lower detection sensitivity. The lower LOD, calculated as 3× the SD at 0 ng/mL divided by the slope of the calibration curve, of this immunosensor for SARS-CoV-2 N protein detection in whole serum and 5× diluted serum is 50 and 10 pg/mL, respectively. We attribute the improved sensitivity obtained from diluted serum compared with whole serum to the use of a commercial assay diluent, which contains blocking agents that inhibit/neutralize the interference of antigen−antibody binding caused by endogenous components, such as heterophilic antibodies and human anti-animal antibodies, in the sample matrix.[23−25] Our results are consistent with those reported in prior works, which demonstrate that matrix interference effects in immunoassays can be diminished by using heterophilic antibody blocking agents.[26,27] While a lower LOD can be achieved using 5× diluted serum with a shorter 25 min incubation time, this requires the serum sample to be diluted prior to the measurement. For applications where sample dilution is undesired, whole serum samples can be used requiring a slightly longer (50 min) incubation time to achieve high sensitivity detection. The sensitivity of this immunosensor is within the range of SARS-CoV-2 N protein serum levels in individuals infected with COVID-19 (1 pg to >10,000 pg/mL[13,14,28]), suggesting that it will be suitable as a diagnostic tool for the detection of COVID-19 infection.

The specificity of this immunosensor was evaluated by performing measurements of whole serum samples spiked with 1 ng/mL of SARS-CoV-2 Spike RBD, another biomarker of


https://dx.doi.org/10.1021/acssensors.0c02561
ACS Sens. XXXX, XXX, XXX−XXX

COVID-19 infection, SARS-CoV N protein, MERS-CoV N protein, and nonspiked serum. As shown in Figure 3C, the amperometric signals generated from the samples containing SARS-CoV-2 Spike RBD and MERS-CoV N protein are similar to the nonspiked serum sample (blank control), indicating that these protein biomarkers do not cross-react with this immunosensor. The amperometric signal from the sample containing SARS-CoV N protein is ~1.5× larger than the background signal, indicating moderate cross-reactivity with the SARS-CoV-2 N protein antibody used in this assay. This is due to >90% conserved similarity in protein sequences between SARS-CoV-2 and SARS-CoV.[29] While cross-reactivity between SARS-CoV N protein and SARS-CoV-2 N antibodies has been previously reported[17] and is an issue for all immunoassays utilizing SARS-CoV-2 N protein antibodies, its impact on the current COVID-19 pandemic is negligible because the number of individuals infected with SARS-CoV is very small compared with SARS-CoV-2 and no new SARS-CoV outbreaks have been reported for nearly two decades.[17,30,31]

**SARS-CoV-2 N Protein Detection Using a Smartphone.** To enhance the portability and simplicity of this immunosensor, we also developed a handheld diagnostic device for quantitative measurements of SARS-CoV-2 N protein in serum. As shown in Figure 4A, this device consists of a Google Pixel 2 smartphone, Sensit Smart potentiostat, and microfluidic immunosensor chip. The microfluidic chip incorporates a waste reservoir to store the liquid samples after being dispensed into the chip (Figure 4B). The sample, wash buffer, and TMB substrate are sequentially dispensed into the chip using capillary tubes and plungers, which circumvents the need for an external pump and power source. We observed that the washing effectiveness using a capillary tube and plunger is lower than that using a syringe pump, which can diminish the detection sensitivity and/or sensor reproducibility. Therefore, an additional step was added to purge the microchamber with air using a 1 cc plastic syringe after each liquid loading step to enhance the removal of unbound DMBs and nonspecific species from the sensor. To evaluate the analytical performance of this device, electrochemical measurements were performed using whole serum and 5× diluted serum samples spiked with increasing concentrations of SARS-CoV-2 N protein. Calibration plots for whole serum and 5× diluted serum samples are presented in Figure 4C, which exhibit excellent linearity with $R^2$ correlation coefficients of 0.9906 and 0.9972, respectively. The lower LOD calculated for whole serum and 5× diluted serum samples is 230 pg/mL and 100 pg/mL, respectively. The detection sensitivity obtained using the smartphone-based device is lower than that using the PalmSens4-based sensing platform because of the reduced effectiveness of the capillary tube and plunger to fully rinse the sensor surface. However, the sensitivity of the handheld device is much higher compared with rapid COVID-19 antigen tests, while offering similar portability, simplicity, and speed, making it useful for point-of-care testing.

**SARS-CoV-2 N Protein Detection in Clinical Serum Specimens.** To evaluate the utility of this immunosensor for diagnosing COVID-19 infection, measurements were performed using serum samples obtained from COVID-19 patients confirmed by RT-PCR ($P_1$−$P_7$) and from healthy, uninfected individuals ($N_1$−$N_4$). Samples $N_1$−$N_3$ were collected pre-COVID-19 from healthy volunteers and sample $N_4$ was obtained from an individual with a negative PCR COVID-19 test result. As shown in Figure 5A, the electrochemical signals generated from specimens obtained from

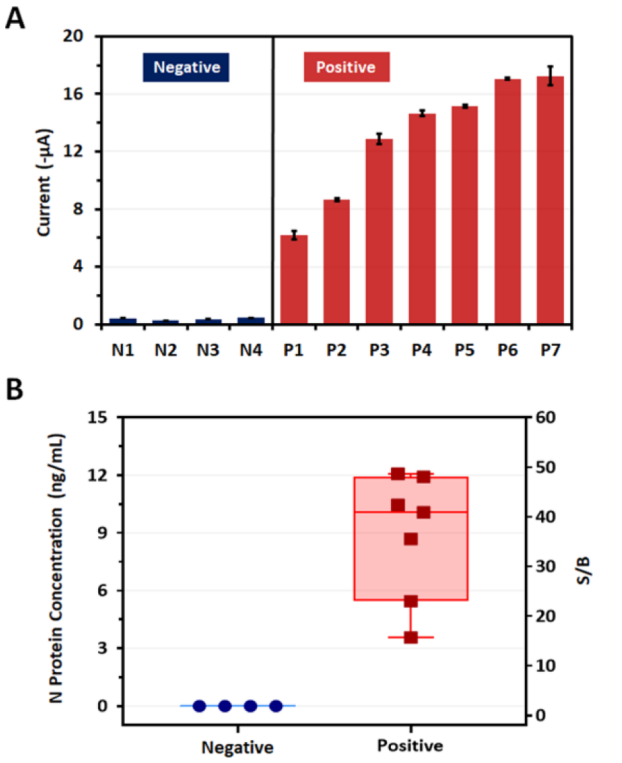


**Figure 5.** (A) Electrochemical signals generated from serum specimens obtained from COVID-19 patients (positive) and uninfected individuals (negative). Each bar represents the mean ± SD of three separate measurements obtained using new sensors. (B) Calculated SARS-CoV-2 N protein concentration and corresponding S/B ratios for clinical serum specimens.

uninfected individuals ($N_1$−$N_4$) are very low (<1 μA). In contrast, the electrochemical signals generated from the specimens obtained from COVID-19 patients are at least 5× larger, ranging from ~5 to 17 μA, which is consistent with the PCR results. Using the calibration plot in Figure 3B, the calculated SARS-CoV-2 N protein concentration and corresponding S/B ratios were determined for the clinical specimens. The data was normalized so that the lowest calculated N protein concentration (which was a negative value) was set to 0 ng/mL (and 1 for the S/B ratio). As shown in Figure 5B, the calculated levels of SARS-CoV-2 N protein in COVID-19 positive specimens range from ~3 to 12 ng/mL, which is consistent with those measured by Torrente-Rodríguez et al. using a graphene-based immunosensor.[17] Based on these preliminary results, this immunosensor can accurately distinguish COVID-19 patients from healthy, uninfected individuals based on SARS-CoV-2 N protein serum levels, demonstrating its usefulness as a diagnostic test for COVID-19.

## CONCLUSIONS

We present a microfluidic immunosensor for rapid, high sensitivity measurements of SARS-CoV-2 N protein in serum. This assay utilizes a unique sensing scheme employing DMBs for immunomagnetic enrichment and signal amplification based on a simple magnetic enrichment process. The analytical performance of this assay was evaluated by performing


https://dx.doi.org/10.1021/acssensors.0c02561
ACS Sens. XXXX, XXX, XXX−XXX

measurements of human serum samples spiked with SARS-CoV-2 N protein, which could be detected at concentrations as low as 10 pg/mL in 5× diluted serum within 30 min and 50 pg/mL in whole serum within 55 min. This immunosensor was also adapted for a smartphone-based diagnostic device, which does not require external pumps or power sources. Using this handheld device, SARS-CoV-2 N protein could be detected in 5× diluted serum and whole serum samples at concentrations as low as 100 and 230 pg/mL, respectively. We also assessed the utility of this immunosensor to detect COVID-19 infection by testing clinical serum specimens, which revealed that it can accurately distinguish PCR-positive COVID-19 patients from healthy, uninfected individuals based on SARS-CoV-2 N protein serum levels. The portability, simplicity, and high sensitivity of this immunosensor makes it a promising tool for point-of-care COVID-19 testing.

## ■ ASSOCIATED CONTENT

### Supporting Information

The Supporting Information is available free of charge at https://pubs.acs.org/doi/10.1021/acssensors.0c02561.

Amperometric signals and S/B ratios generated from serum samples spiked with SARS-CoV-2 N protein using a microfluidic immunosensor and an open-well immunosensor (PDF)

## ■ AUTHOR INFORMATION


### Corresponding Author

**Peter B. Lillehoj** − *Department of Mechanical Engineering and Department of Bioengineering, Rice University, Houston, Texas 77005, United States;* orcid.org/0000-0002-0289-2634; Email: lillehoj@rice.edu

### Author

**Jiran Li** − *Department of Mechanical Engineering, Rice University, Houston, Texas 77005, United States*

Complete contact information is available at: https://pubs.acs.org/10.1021/acssensors.0c02561


### Notes

The authors declare no competing financial interest.

## ■ ACKNOWLEDGMENTS

This work was supported by the National Institutes of Health (R01AI113257), the National Science Foundation (Award # 1350560), and COVID-19 research funding from Rice University. We thank Advaite, Inc. for providing us with SARS-CoV-2 nucleocapsid protein.

## ■ REFERENCES


(1) COVID-19 Map - Johns Hopkins Coronavirus Resource Center. https://coronavirus.jhu.edu/map.html (accessed Nov 8, 2020).

(2) Zhang, W.; Du, R.-H.; Li, B.; Zheng, X.-S.; Yang, X.-L.; Hu, B.; Wang, Y.-Y.; Xiao, G.-F.; Yan, B.; Shi, Z.-L.; Zhou, P. Molecular and Serological Investigation of 2019-NCoV Infected Patients: Implication of Multiple Shedding Routes. *Emerg. Microb. Infect.* **2020**, *9*, 386−389.

(3) Fang, Y.; Zhang, H.; Xie, J.; Lin, M.; Ying, L.; Pang, P.; Ji, W. Sensitivity of Chest CT for COVID-19: Comparison to RT-PCR. *Radiology* **2020**, *296*, E115−E117.

(4) Wölfel, R.; Corman, V. M.; Guggemos, W.; Seilmaier, M.; Zange, S.; Müller, M. A.; Niemeyer, D.; Jones, T. C.; Vollmar, P.; Rothe, C.; Hoelscher, M.; Bleicker, T.; Brünink, S.; Schneider, J.; Ehmann, R.; Zwirglmaier, K.; Drosten, C.; Wendtner, C. Virological Assessment of Hospitalized Patients with COVID-2019. *Nature* **2020**, *581*, 465−469.

(5) West, C. P.; Montori, V. M.; Sampathkumar, P. COVID-19 Testing: The Threat of False-Negative Results. *Mayo Clinic Proceedings*; Elsevier Ltd, June 1, 2020; Vol. *95*, pp 1127−1129.

(6) Xiao, S. Y.; Wu, Y.; Liu, H. Evolving Status of the 2019 Novel Coronavirus Infection: Proposal of Conventional Serologic Assays for Disease Diagnosis and Infection Monitoring. *J. Med. Virol.* **2020**, *92*, 464−467.

(7) Guo, L.; Ren, L.; Yang, S.; Xiao, M.; Chang, D.; Yang, F.; Dela Cruz, C. S.; Wang, Y.; Wu, C.; Xiao, Y.; Zhang, L.; Han, L.; Dang, S.; Xu, Y.; Yang, Q.-W.; Xu, S.-Y.; Zhu, H.-D.; Xu, Y.-C.; Jin, Q.; Sharma, L.; Wang, L.; Wang, J. Profiling Early Humoral Response to Diagnose Novel Coronavirus Disease (COVID-19). *Clin. Infect. Dis.* **2020**, *71*, 778−785.

(8) Liu, W.; Liu, L.; Kou, G.; Zheng, Y.; Ding, Y.; Ni, W.; Wang, Q.; Tan, L.; Wu, W.; Tang, S.; Xiong, Z.; Zheng, S. Evaluation of Nucleocapsid and Spike Protein-Based Enzyme-Linked Immunosorbent Assays for Detecting Antibodies against SARS-CoV-2. *J. Clin. Microbiol.* **2020**, *58*, No. e00461.

(9) Zhao, J.; Yuan, Q.; Wang, H.; Liu, W.; Liao, X.; Su, Y.; Wang, X.; Yuan, J.; Li, T.; Li, J.; Qian, S.; Hong, C.; Wang, F.; Liu, Y.; Wang, Z.; He, Q.; Li, Z.; He, B.; Zhang, T.; Fu, Y.; Ge, S.; Liu, L.; Zhang, J.; Xia, N.; Zhang, Z. Antibody Responses to SARS-CoV-2 in Patients With Novel Coronavirus Disease 2019. *Clin. Infect. Dis.* **2020**, *71*, 2027−2034.

(10) Xiang, J.; Yan, M.; Li, H.; Liu, T.; Lin, C.; Huang, S.; Shen, C. Evaluation of Enzyme-Linked Immunoassay and Colloidal Gold-Immunochromatographic Assay Kit for Detection of Novel Coronavirus (SARS-Cov-2) Causing an Outbreak of Pneumonia (COVID-19). **2020**, medRxiv 2020.02.27.20028787.

(11) Li, Z.; Yi, Y.; Luo, X.; Xiong, N.; Liu, Y.; Li, S.; Sun, R.; Wang, Y.; Hu, B.; Chen, W.; Zhang, Y.; Wang, J.; Huang, B.; Lin, Y.; Yang, J.; Cai, W.; Wang, X.; Cheng, J.; Chen, Z.; Sun, K.; Pan, W.; Zhan, Z.; Chen, L.; Ye, F. Development and clinical application of a rapid IgM-IgG combined antibody test for SARS-CoV-2 infection diagnosis. *J. Med. Virol.* **2020**, *92*, 1518−1524.

(12) Tomaras, G. D.; Haynes, B. F. HIV-1-specific antibody responses during acute and chronic HIV-1 infection. *Curr Opin HIV AIDS.* **2009**, *4*, 373−379.

(13) Li, T.; Wang, L.; Wang, H.; Li, X.; Zhang, S.; Xu, Y.; Wei, W. Serum SARS-COV-2 Nucleocapsid Protein: A Sensitivity and Specificity Early Diagnostic Marker for SARS-COV-2 Infection. *Front. Cell. Infect. Microbiol.* **2020**, *10*, 470.

(14) Ogata, A. F.; Maley, A. M.; Wu, C.; Gilboa, T.; Norman, M.; Lazarovits, R.; Mao, C.-P.; Newton, G.; Chang, M.; Nguyen, K.; Kamkaew, M.; Zhu, Q.; Gibson, T. E.; Ryan, E. T.; Charles, R. C.; Marasco, W. A.; Walt, D. R. Ultra-Sensitive Serial Profiling of SARS-CoV-2 Antigens and Antibodies in Plasma to Understand Disease Progression in COVID-19 Patients with Severe Disease. *Clin. Chem.* **2020**, *66*, 1562.

(15) Fabiani, L.; Saroglia, M.; Galatà, G.; De Santis, R.; Fillo, S.; Luca, V.; Faggioni, G.; D'Amore, N.; Regalbuto, E.; Salvatori, P.; Terova, G.; Moscone, D.; Lista, F.; Arduini, F. Magnetic Beads Combined with Carbon Black-Based Screen-Printed Electrodes for COVID-19: A Reliable and Miniaturized Electrochemical Immunosensor for SARS-CoV-2 Detection in Saliva. *Biosens. Bioelectron.* **2021**, *171*, 112686.

(16) Tan, X.; Krel, M.; Dolgov, E.; Park, S.; Li, X.; Wu, W.; Sun, Y.-L.; Zhang, J.; Khaing Oo, M. K.; Perlin, D. S.; Fan, X. Rapid and Quantitative Detection of SARS-CoV-2 Specific IgG for Convalescent Serum Evaluation. *Biosens. Bioelectron.* **2020**, *169*, 112572.

(17) Torrente-Rodríguez, R. M.; Lukas, H.; Tu, J.; Min, J.; Yang, Y.; Xu, C.; Rossiter, H. B.; Gao, W. SARS-CoV-2 RapidPlex: A Graphene-Based Multiplexed Telemedicine Platform for Rapid and Low-Cost COVID-19 Diagnosis and Monitoring. *Matter* **2020**, *3*, 1981−1998.

(18) Ng, A. H. C.; Uddayasankar, U.; Wheeler, A. R. Immunoassays in Microfluidic Systems. *Analytical and Bioanalytical Chemistry*; Springer June 27, 2010, pp 991−1007.
(19) Choi, C. J.; Belobraydich, A. R.; Chan, L. L.; Mathias, P. C.; Cunningham, B. T. Comparison of Label-Free Biosensing in Microplate, Microfluidic, and Spot-Based Affinity Capture Assays. *Anal. Biochem.* **2010**, *145*, 1.
(20) Min, J.; Nothing, M.; Coble, B.; Zheng, H.; Park, J.; Im, H.; Weber, G. F.; Castro, C. M.; Swirski, F. K.; Weissleder, R.; Lee, H. Integrated Biosensor for Rapid and Point-of-Care Sepsis Diagnosis. *ACS Nano* **2018**, *12*, 3378−3384.
(21) Valverde, A.; Serafín, V.; Garoz, J.; Montero-Calle, A.; González-Cortés, A.; Arenas, M.; Camps, J.; Barderas, R.; Yáñez-Sedeño, P.; Campuzano, S.; Pingarrón, J. M. Electrochemical Immunoplatform to Improve the Reliability of Breast Cancer Diagnosis through the Simultaneous Determination of RANKL and TNF in Serum. *Sens. Actuators, B* **2020**, *314*, 128096.
(22) Otieno, B. A.; Krause, C. E.; Jones, A. L.; Kremer, R. B.; Rusling, J. F. Cancer Diagnostics via Ultrasensitive Multiplexed Detection of Parathyroid Hormone-Related Peptides with a Microfluidic Immunoarray. *Anal. Chem.* **2016**, *88*, 9269−9275.
(23) Tate, J.; Ward, G. Interferences in Immunoassay. *Clin. Biochem. Rev.* **2004**, *25*, 105−120.
(24) Kricka, L. J. Human Anti-Animal Antibody Interferences in Immunological Assays. *Clin. Chem.* **1999**, *45*, 942−956.
(25) Spengler, M.; Adler, M.; Niemeyer, C. M. Highly Sensitive Ligand-Binding Assays in Pre-Clinical and Clinical Applications: Immuno-PCR and Other Emerging Techniques. *Analyst* **2015**, *140*, 6175−6194.
(26) DeForge, L. E.; Loyet, K. M.; Delarosa, D.; Chinn, J.; Zamanian, F.; Chuntharapai, A.; Lee, J.; Hass, P.; Wei, N.; Townsend, M. J.; Wang, J.; Wong, W. L. T. Evaluation of Heterophilic Antibody Blocking Agents in Reducing False Positive Interference in Immunoassays for IL-17AA, IL-17FF, and IL-17AF. *J. Immunol. Methods* **2010**, *362*, 70−81.
(27) Nicholson, S.; Fox, M.; Epenetos, A.; Rustin, G. Immunoglobulin Ihhibiting Reagent: Evaluation of a New Method for Eliminating Spurious Elevations in CA125 Caused by HAMA. *Int. J. Biol. Markers* **1996**, *11*, 46−49.
(28) Shan, D.; Johnson, J. M.; Fernandes, S. C.; Mendes, M.; Suib, H.; Holdridge, M.; Burke, E. M.; Beauregard, K.; Zhang, Y.; Cleary, M.; Xu, S.; Yao, X.; Patel, P.; Plavina, T.; Wilson, D.; Chang, L.; Kaiser, K. M.; Natterman, J.; Schmidt, S. V.; Latz, E.; Hrusovsky, K.; Mattoon, D.; Ball, A. J. SARS-Coronavirus-2 nucleocapsid protein measured in blood using a Simoa ultra-sensitive immunoassay differentiates COVID-19 infection with high clinical sensitivity. **2020**, medRxiv: 2020.08.14.20175356.
(29) Zeng, W.; Liu, G.; Ma, H.; Zhao, D.; Yang, Y.; Liu, M.; Mohammed, A.; Zhao, C.; Yang, Y.; Xie, J.; Ding, C.; Ma, X.; Weng, J.; Gao, Y.; He, H.; Jin, T. Biochemical Characterization of SARS-CoV-2 Nucleocapsid Protein. *Biochem. Biophys. Res. Commun.* **2020**, *527*, 618−623.
(30) Shrock, E.; Fujimura, E.; Kula, T.; Timms, R. T.; Lee, I.-H.; Leng, Y.; Robinson, M. L.; Sie, B. M.; Li, M. Z.; Chen, Y.; Logue, J.; Zuiani, A.; McCulloch, D.; Lelis, F. J. N.; Henson, S.; Monaco, D. R.; Travers, M.; Habibi, S.; Clarke, W. A.; Caturegli, P.; Laeyendecker, O.; Piechocka-Trocha, A.; Li, J. Z.; Khatri, A.; Chu, H. Y.; Villani, A.-C.; Kays, K.; Goldberg, M. B.; Hacohen, N.; Filbin, M. R.; Yu, X. G.; Walker, B. D.; Wesemann, D. R.; Larman, H. B.; Lederer, J. A.; Elledge, S. J. Viral Epitope Profiling of COVID-19 Patients Reveals Cross-Reactivity and Correlates of Severity. *Science* **2020**, *370*, No. eabd4250.
(31) Ma, Z.; Li, P.; Ji, Y.; Ikram, A.; Pan, Q. Cross-Reactivity towards SARS-CoV-2: The Potential Role of Low-Pathogenic Human Coronaviruses. *Lancet Microbe* **2020**, *1*, No. e151.


https://dx.doi.org/10.1021/acssensors.0c02561
*ACS Sens.* XXXX, XXX, XXX−XXX